

Gas-Phase Collision-Induced Dissociation of Highly Excited NO<sub>2</sub>

C. R. Bieler, A. Sanov, M. Hunter, and H. Reisler\*

Department of Chemistry, University of Southern California, Los Angeles, California 90089-0482

Received: November 30, 1993\*

The gas-phase collision-induced dissociation (CID) of highly excited NO<sub>2</sub> with argon has been observed in a crossed beams experiment. The dissociation yield as a function of the initial NO<sub>2</sub> excitation energy is reported. The structure of the CID signal is similar to that observed in the fluorescence excitation spectrum of NO<sub>2</sub>, and the scaling of energy transfer can be described by an exponential decay law. NO is detected state selectively using laser ionization, and state distributions are determined.

## Introduction

Gas-phase collision-induced dissociation (CID) is an important process in unimolecular decomposition induced by collisional energy transfer. CID of ions has been routinely utilized in tandem mass spectrometry<sup>1</sup> and in the determination of sequential bond energies,<sup>2</sup> ion fragmentation processes, and ion structure.<sup>1,3</sup> In these applications the use of ions allows for the efficient and extensive acceleration of incident particles. In contrast, few studies of CID have been performed on neutrals primarily due to the difficulty in achieving, under well-defined conditions, the chemically significant collision energies necessary for ground-state dissociation.

For heavy incident neutral molecules, aerodynamic acceleration is the method of choice for production of hypersonic molecules with several electronvolts of translational energy. Tully et al.<sup>4</sup> and Wexler and co-workers<sup>5</sup> have observed CID of alkali halides with rare gas colliders at collision energies up to 6 eV. This energy is sufficient to cause dissociation to ion pairs. Related CID experiments have been performed on surfaces.<sup>6,7</sup> For example, NO products were detected state selectively in the CID of C<sub>3</sub>F<sub>7</sub>NO on MgO(100).<sup>6</sup> Finally, laser excitation into upper electronic states was used by Leone and co-workers<sup>8</sup> to study the CID of Br<sub>2</sub>. Collisions of the excited species caused a nonadiabatic electronic predissociation via a nearby repulsive electronic surface. However, the lifetimes of these species are rather short (nanoseconds), and the experiments that can be performed with them are limited.

Understanding the behavior of highly vibrationally excited molecules in collisional environments is also of fundamental importance to chemical change. In addition to CID, these molecules may undergo chemical reactions and collisional relaxation. Here, we report our first studies of the effects of collisions on highly internally excited NO<sub>2</sub> by observing its CID. These studies are carried out under single-collision conditions in pulsed molecular beams and with well-defined translational energies of the colliders. The NO products are detected state selectively. The ability to vary the initial internal energy of the reactant, the relative collision energy, and the monitored quantum state of the NO product allows detailed studies of energy transfer.

NO<sub>2</sub> is easily excited into long-lived highly internally excited states, and its CID process is shown schematically in Figure 1. It is excited to energies less than a few hundred wavenumbers below dissociation threshold ( $D_0 = 25\,130\text{ cm}^{-1}$ ) via the well-known  ${}^2B_2 \leftarrow X^2A_1$  transition. The mixing between the ground  ${}^2A_1$  and excited  ${}^2B_2$  electronic states of NO<sub>2</sub> results in strongly mixed  ${}^2B_2/{}^2A_1$  eigenstates,<sup>9,10</sup> with predominantly ground-state character, which have lifetimes of  $\geq 50\ \mu\text{s}$ .<sup>11</sup> Collisions between argon and the excited NO<sub>2</sub> can cause, among other processes, T

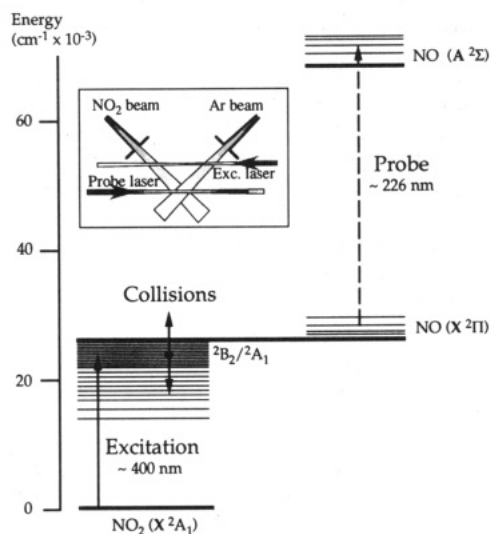


**Figure 1.** Energy level diagram depicting the CID reaction scheme. The first step includes the excitation of NO<sub>2</sub> to energy states just below  $D_0$ . Collision with an argon atom transfers energy to the NO<sub>2</sub> molecule, placing it above  $D_0$ , and the molecule dissociates to form NO( $X^2\Pi$ ) and O( ${}^3P$ ). The inset shows the experimental arrangement of the molecular and laser beams.

→ V energy transfer which can promote the excited NO<sub>2</sub> molecules to levels above  $D_0$  resulting in dissociation to NO( ${}^2\Pi$ ) + O( ${}^3P$ ). NO products are detected by laser ionization, thereby allowing us to obtain state distributions and to estimate the relative efficiency of CID as a function of the internal energy in NO<sub>2</sub>.

## Experimental Section

The experiments are performed in a dual crossed beams apparatus in which the two beams are differentially pumped and skimmed. The pulsed molecular beams ( $\sim 150\text{-}\mu\text{s}$  duration) travel approximately 5 cm from the skimmer to the center of the chamber and intersect at  $90^\circ$ , creating an overlap region of  $\sim 5\text{ mm}^3$ . The first beam consists of a 5% NO<sub>2</sub>/5% O<sub>2</sub> mixture in helium carrier, and the second beam is neat argon. The NO<sub>2</sub> gas mixture is prepared as described previously.<sup>12</sup> The vacuum chamber base pressure is  $\sim 5 \times 10^{-7}$  Torr, and under typical operating conditions (10-Hz pulse repetition rate, 1-atm backing pressure in both nozzles) the pressure in the collision chamber is  $< 10^{-5}$  Torr. The relative collision energy of the NO<sub>2</sub>/Ar system is  $1850\text{ cm}^{-1}$ , as estimated for fully expanded seeded beams,<sup>13</sup> and the energy spread is  $\sim 10\%$ . A rough estimate of the mean free path of the NO<sub>2</sub> molecules in the collision region, obtained by considering the expected number densities in the supersonic molecular beams, indicates that these experiments are performed under nearly single-collision conditions. A TOF spectrometer of the Wiley-McLaren

\* Abstract published in *Advance ACS Abstracts*, January 15, 1994.

design is positioned above the center of the chamber to allow for the mass selection of ions, and a microchannel plate is used for ion detection. Two excimer pumped dye lasers are utilized as the excitation and probe radiation sources. The laser beams are loosely focused with 1-m-focal length lenses to approximately 2-mm spot sizes and counterpropagate through the center of the chamber in the plane of the molecular beams, intersecting them at 45° and 135°. The excitation laser beam (~400 nm, 15-ns duration, pulse energy ≈4 mJ) intersects the NO<sub>2</sub> beam 3 cm before the center of the collision region (see inset in Figure 1). The probe dye laser output (~226 nm, 15 ns, pulse energy ≈150 μJ) is located at the center of the collision region, and NO is detected by resonant 1 + 1 multiphoton ionization (REMPI) via the A<sup>2</sup>Σ<sup>+</sup> ← X<sup>2</sup>Π transition. NO distributions were extracted from the REMPI spectra by assuming that the transitions are saturated. The delay between the excitation and the probe laser pulses must be set at  $\tau = 20.0 \pm 0.5 \mu\text{s}$  in order to observe the CID signal. This is due to the fact that the excited NO<sub>2</sub> molecules in the supersonic molecular beam travel 3 cm from the excitation to the collision region. The long lifetime of the excited states of NO<sub>2</sub> enables them to travel this distance.

There are several competing processes and background signals that must be considered. First, owing to the surface-catalyzed decomposition of NO<sub>2</sub>, small NO concentrations are always present in the molecular beam. To subtract the background signal due to the collisional (rotationally inelastic) scattering of the NO contaminant, both the Ar beam pulsed nozzle and the excitation laser were operated in an on/off mode. The CID signal was extracted by subtracting the collision-induced signal obtained with the excitation laser off (i.e., the scattered NO contaminant) from the total collision-induced signal obtained with the excitation laser on. Second, to decrease the likelihood of photodissociation of collisionally excited NO<sub>2</sub>, the NO<sub>2</sub> was excited *before* the molecules entered the collision region. To achieve this, the excitation laser beam was positioned 3 cm from the center of the chamber upstream along the NO<sub>2</sub> beam, a position which is well outside the molecular beams intersection region (see the inset of Figure 1).

Last, the contribution from multiphoton processes had to be taken into account. Despite the fact that the lasers fluences were low, several multiphoton processes were evident due to the large absorption cross section of the excited NO<sub>2</sub>. First, the signal due to the multiphoton ionization of NO<sub>2</sub> was eliminated by setting the TOF spectrometer to monitor only NO<sup>+</sup> ions. Second, NO signals arising from multiphoton dissociation of NO<sub>2</sub> by the excitation laser were minimized by discriminating against NO formed at the excitation region. Since any NO created by two-photon dissociation has substantial translational energy, it will recoil out of the molecular beam before it reaches the collision region. Finally, we observed a two-color, two-photon (400 + 226 nm) dissociation of NO<sub>2</sub> which yielded NO(A<sup>2</sup>Σ<sup>+</sup>). This process can be prevented by keeping the laser wavelengths below the NO<sub>2</sub> → NO(A<sup>2</sup>Σ<sup>+</sup>) + O(<sup>3</sup>P) dissociation threshold. Because of the nonresonant nature of the ionization of electronically excited NO(A<sup>2</sup>Σ<sup>+</sup>), this process does not give rise to a structured absorption feature and leads to a nearly constant background signal at higher probe energies.

## Results and Discussion

Figure 2 shows the dependence of the CID signal intensity on the initial vibrational excitation energy of NO<sub>2</sub>. This spectrum was obtained by scanning the wavelength of the excitation laser below the NO<sub>2</sub> dissociation threshold while the probe laser monitored the production of NO(X<sup>2</sup>Π<sub>1/2</sub>; v=0; J=5.5). The CID signal was observed at excitation energies from a few cm<sup>-1</sup> to ~600 cm<sup>-1</sup> below D<sub>0</sub> with the intensity of the signal decreasing exponentially as the excitation laser energy is decreased. This type of scaling has been observed previously for several systems<sup>14</sup>

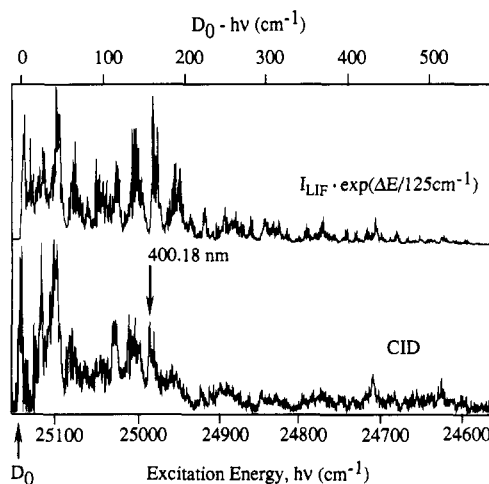


**Figure 2.** NO CID fragment yield spectrum and exponentially weighted NO<sub>2</sub> LIF spectrum obtained by scanning the NO<sub>2</sub> initial excitation energy below D<sub>0</sub>. For the CID spectrum, the probe laser was positioned to detect production of NO(X<sup>2</sup>Π<sub>1/2</sub>; v=0; J=5.5).

and is consistent with the exponential energy gap law for energy transfer.<sup>15</sup> Similar spectra were observed when probing other product NO rotational states.

A key observation in identifying the origin of the NO signal is the structure apparent in the CID yield spectrum which is very similar to that observed in the NO<sub>2</sub> laser-induced fluorescence (LIF) spectrum. This is the primary indication that what is observed is in fact a process involving absorption into excited states of NO<sub>2</sub> from jet-cooled ( $T_{\text{rot}} \approx 5 \text{ K}$ ) NO<sub>2</sub>. When the excitation laser interacts with NO<sub>2</sub> that has been rotationally excited by collisions (for example, when the laser excitation takes place in the collision region), NO is produced mainly by photodissociation, and no structure in the NO yield spectrum is observed. For comparison with CID, an example of the NO<sub>2</sub> LIF spectrum, taken in a companion molecular beam chamber using the same excitation laser, is also shown in Figure 2, and the similarities are apparent. Notice that the plotted relative intensities in the LIF spectrum,  $I$ , are weighted by an exponential decay relative to the intensity of the LIF peaks,  $I_{\text{LIF}}$ , to account for the decrease in energy-transfer efficiency in the CID experiments,

$$I = I_{\text{LIF}} \exp(-|E_i - E_f|/\beta)$$

In the region 0–400 cm<sup>-1</sup> below D<sub>0</sub> the least-squares fit to the CID spectrum was found to give a value for  $\beta$  of  $125 \pm 10 \text{ cm}^{-1}$ . It should be noted that in order to make such an estimate for a wider energy range the intensity of the CID signal must be normalized to the total yield of NO<sub>2</sub> CID, since in this experiment only the fractional population of the NO product in the  $J = 5.5$  rotational state is monitored. As will be discussed, over this narrow energy range the fractional population of  $J = 5.5$  did not change significantly. Assuming an exponential gap scaling law,  $\beta$  is a measure of the average energy transferred per collision. Comparisons to previously observed T → V energy-transfer processes for small systems reveal a good agreement in the value of the  $\beta$  parameter. For instance, a value of 100 cm<sup>-1</sup> for the T → V energy transfer was obtained in I<sub>2</sub>(B) + He experiments.<sup>16</sup>

The CID near D<sub>0</sub> proved to be quite efficient. Assuming comparable absorption cross sections, it is found that when probing NO( $J=5.5$ ), the CID signal just below D<sub>0</sub> is ~5% of the photodissociation signal near the threshold of formation of NO( $J=5.5$ ). This is a significant amount, taking into account that for photodissociation the energy is partitioned into six NO rotational states, whereas for CID NO product state distributions show that NO is populated up to  $J = 20.5$ .

Further dynamical aspects relating to the dissociation process can be revealed by studying the NO rotational state distributions.

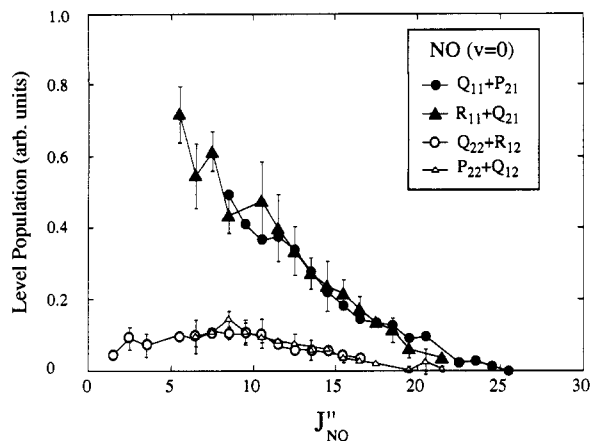


**Figure 3.** NO product state distributions from CID of  $\text{NO}_2$  excited with 400.18-nm radiation ( $160\text{ cm}^{-1}$  below  $D_0$ ). The distributions were extracted from the  $\text{NO } A^2\Sigma^+ \leftarrow X^2\Pi(0,0)$  spectra averaged over 10 runs of the experiment. In each run five laser shots were averaged per data point.

These distributions are obtained by fixing the excitation laser at a specific wavelength below  $D_0$  and scanning the probe laser over the  $\text{NO}(A \leftarrow X)$  transition. Distributions were measured at several excitation wavelengths ranging from  $60$  to  $440\text{ cm}^{-1}$  below  $D_0$ . Figure 3 shows a typical rotational distribution obtained following excitation at  $400.18\text{ nm}$  ( $160\text{ cm}^{-1}$  below  $D_0$ ), where  $1690\text{ cm}^{-1}$  of energy is available to the NO product. Distributions obtained at the other laser excitation energies are quite similar. Taking into account the value of the collision energy,  $1850\text{ cm}^{-1}$ , the energy available to the NO CID product does not vary considerably within the studied energy range (i.e., from  $1790$  to  $1410\text{ cm}^{-1}$ ), and a large change in the product distribution is not expected within the signal/noise ratio of our measurements. However, assuming an exponential scaling law for energy transfer, it is noteworthy that NO is populated to such high  $J$ 's even at the relatively low collisional energy of this experiment. This may suggest some interaction among the collision partners in the exit channel.

Support for such an interpretation is found by the good fit of the exponentially weighted LIF spectrum to the CID spectrum (Figure 2), which suggests an adiabatic nature of the interaction.<sup>17</sup> The adiabatic regime assumes long collision times compared to the vibrational period of  $\text{NO}_2$  and may even lead to "chattering" collisions.<sup>18</sup> We note that in ion CID experiments even at higher collisional energies (e.g. several electronvolts, as compared to  $0.23\text{ eV}$  in the present experiment), when the impulsive collision time is expected to be much shorter, formation of a collision

complex leading to efficient energy transfer was observed.<sup>19</sup> However, the cold spin-orbit population of the NO product would mitigate against a collision time sufficiently long to allow for equilibration of the two spin-orbit states. Very recent results on the CID of vibrationally excited  $\text{NO}_2$  on  $\text{MgO}(100)$  surface at comparable relative energies gave rise to rotational distributions similar to those observed in the gas-phase CID, but with equally populated spin-orbit states.<sup>20</sup> Thus, the spin-orbit ratio may serve as a sensitive probe of the details of the interaction potential.

More work is clearly needed to probe these interesting processes. Current work involves CID with polar colliders, as well as more chemically interesting systems where reactions can occur.

**Acknowledgment.** The authors thank Scott Reid for help with the  $\text{NO}_2$  LIF spectrum and Hans Ferkel and Curt Wittig for valuable discussions. This research is supported by the National Science Foundation and the Army Research Office.

## References and Notes

- (1) Busch, K. L.; Glish, G. L.; McLuckey, S. A. *Mass Spectrometry/Mass Spectrometry*; VCH: New York, 1988.
- (2) For example, Khan, F. A.; Clemmer, D. E.; Schultz, R. H.; Armentrout, P. B. *J. Phys. Chem.* **1993**, *97*, 7978.
- (3) Lee, Y. J.; Kim, M. S. *J. Phys. Chem.* **1993**, *97*, 1119 and references therein.
- (4) (a) Tully, F. P.; Lee, Y. T.; Berry, R. S. *Chem. Phys. Lett.* **1971**, *9*, 80. (b) Tully, F. P.; Cheung, W. H.; Haberland, H.; Lee, Y. T. *J. Chem. Phys.* **1980**, *73*, 4460.
- (5) Parks, E. K.; Pobo, L. G.; Wexler, S. J. *J. Chem. Phys.* **1984**, *80*, 5003.
- (6) Kolodney, E.; Powers, P. S.; Hodgson, L.; Reisler, H.; Wittig, C. *J. Chem. Phys.* **1991**, *94*, 2330.
- (7) Danon, A.; Amirav, A. *J. Phys. Chem.* **1989**, *93*, 5549 and references therein.
- (8) Smedley, J. E.; Haugen, H. K.; Leone, S. R. *J. Chem. Phys.* **1987**, *86*, 6801.
- (9) (a) Delon, A.; Jost, R. *J. Chem. Phys.* **1991**, *95*, 5686. (b) Delon, A.; Jost, R.; Lombardi, M. *J. Chem. Phys.* **1991**, *95*, 5701.
- (10) (a) Shibuya, K.; Kusumoto, T.; Nagai, H.; Obi, K. *J. Chem. Phys.* **1991**, *95*, 720. (b) Nagai, H.; Aoki, K.; Kusumoto, T.; Shibuya, K.; Obi, K. *J. Phys. Chem.* **1991**, *95*, 2718.
- (11) Patten, Jr., K. O.; Burley, J. D.; Johnston, H. S. *J. Phys. Chem.* **1990**, *94*, 7960.
- (12) Robie, D. C.; Hunter, M.; Bates, J. L.; Reisler, H. *Chem. Phys. Lett.* **1992**, *193*, 413.
- (13) Kolodney, E.; Amirav, A. *Chem. Phys.* **1983**, *82*, 269.
- (14) For a recent review see: Oref, I.; Tardy, D. C. *Chem. Rev.* **1990**, *90*, 1407.
- (15) Troe, J. *J. Chem. Phys.* **1977**, *66*, 4745.
- (16) (a) Krajnovich, D. J.; Butz, K. W.; Du, H.; Parmenter, C. S. *J. Chem. Phys.* **1989**, *91*, 7705. (b) Krajnovich, D. J.; Butz, K. W.; Du, H.; Parmenter, C. S. *J. Chem. Phys.* **1989**, *91*, 7725.
- (17) Landau, L.; Teller, E. *Phys. Z. Sowjetunion* **1936**, *10*, 34.
- (18) Gilbert, R. G. *Int. Rev. Phys. Chem.* **1991**, *10*, 319.
- (19) Nacson, S.; Harrison, A. G. *Int. J. Mass Spectrom. Ion Processes* **1985**, *63*, 325.
- (20) Ferkel, H.; Singleton, J. T.; Reisler, H.; Wittig, C. Unpublished results.